Fast Charge Separation at Semiconductor Sensitizer−Molecular Relay Interface Leads to Significantly Enhanced Solar Cell Performance

ARTICLE *in* THE JOURNAL OF PHYSICAL CHEMISTRY C · APRIL 2015

Impact Factor: 4.77 · DOI: 10.1021/acs.jpcc.5b03313

8 AUTHORS, INCLUDING:

Chao Shen
National University of Singapore
6 PUBLICATIONS **134** CITATIONS
SEE PROFILE

Zhu Hai
National University of Singapore
8 PUBLICATIONS **22** CITATIONS
SEE PROFILE

Qing-Hua Xu
National University of Singapore
129 PUBLICATIONS **3,346** CITATIONS
SEE PROFILE

Qing Wang
University of Reading
78 PUBLICATIONS **3,846** CITATIONS
SEE PROFILE

THE JOURNAL OF PHYSICAL CHEMISTRY C

Article

pubs.acs.org/JPCC

Fast Charge Separation at Semiconductor Sensitizer−Molecular Relay Interface Leads to Significantly Enhanced Solar Cell Performance

Chao Shen,[†] Xingzhu Wang,[†] Xiao-Fang Jiang,[‡] Hai Zhu,[‡] Feng Li,[†] Jing Yang,[†] Qing-Hua Xu,[‡] and Qing Wang*,[†]

[†]Department of Materials Science and Engineering, Faculty of Engineering, NUSNNI-NanoCore, National University of Singapore, 117576 Singapore

[‡]Department of Chemistry, Faculty of Science, National University of Singapore, 117543 Singapore

Supporting Information

ABSTRACT: We report on an effective strategy to improve the efficiency and stability of liquid junction semiconductor-sensitized solar cells employing cobalt bipyridyl complex-based electrolyte. With CdS-sensitized TiO_2 as a model system, we demonstrate that grafting the surface of CdS with small relay molecule, 4′-(bis(4-(hexyloxy)phenyl)amino)-biphenyl-4-carboxylic acid (PAPC), drastically improves the cell performance and leads to an unprecedented power conversion efficiency. Transient absorption measurement indicates the photogenerated holes in CdS could be instantaneously intercepted by the grafted PAPC molecules, which greatly facilitates the charge separation and thus stabilizes CdS. We believe such a concept could be applied to other semiconductor sensitizers, especially for those with superior light absorption, such as CdSe, CdTe, etc.

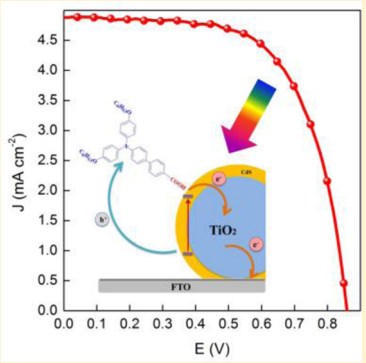

Semiconductor-sensitized solar cells (SSCs) have attracted great attention due to their potential for developing next-generation devices for highly efficient solar energy conversion.[1−4] Compared to their dye-sensitized counterpart,[5−8] narrow band gap semiconductors, also known as quantum dots (QDs), exhibit several advantages for light harvesting and photon conversion, such as high extinction coefficient,[9] tunable light absorption, multiple exciton generation effects (MEG),[10,11] etc. However, one critical issue for SSC is the poor stability of liquid junction devices, resulting from dissolution of sensitizer in electrolyte.[12] Therefore, a polysulfide electrolyte is generally employed due to its compatibility with sensitizers and superior hole extraction ability from the valence band of QDs.[13,14] While the power conversion efficiency of SSC has reached above 5%,[15,16] it still lags far behind its molecular sensitizer counterpart. The main reason for the low power conversion efficiency for SSCs is the relatively low open circuit photovoltage (V_{OC}) and fill factor (FF), which are largely limited by the very negative redox potential of the polysulfide redox mediator (∼−0.67 V vs Ag/AgCl)[17] and the sluggish reaction rate of polysulfide at the counter electrode. Hence, to further enhance the cell performance, noncorrosive redox mediators with more positive redox potential and fast kinetics at counter electrode should be employed in place of polysulfide, so that both V_{OC} and FF could be improved.

Of various redox mediators studied to date, cobalt−bipyridyl complexes seem to be interesting in several aspects. Their redox potentials are generally more positive than polysulfide, for instance 0.56 V vs NHE for $[Co(bpy)_3]^{2+/3+}$.[18] In addition, platinized FTO counter electrode exhibits excellent catalytic property toward cobalt complex-based electrolyte, making it possible to obtain good FF. Cobalt−bipyridyl complexes have been successfully employed in dye-sensitized solar cells (DSCs)[7,19,20] and achieved 13% efficiency with a V_{OC} of 0.91 V.[8] There have been attempts to employ cobalt complexes in SSCs. Unfortunately, the cells suffered from severe photocorrosion and fast recombination and thus poor performance.[21] To address the issues, one should remove holes instantaneously from the semiconductors sensitizer after electron injection as the polysulfide does and suppress the fast recombination of the injected electrons with cobalt complex in the electrolyte. To overcome the instability problems, people have tried to protect the surface of TiO_2/QDs film with large band gap metal oxide, such as Al_2O_3[22] or TiO_2,[23] which however forms an energy barrier for hole separation. Small molecules with negative dipole moment have also been investigated, but the improvement of solar performance is limited.[24,25] Alternatively, organic dyes with suitable energy levels and complementary absorption were adsorbed on the surface of QDs.[26] Yet because of the complexity and inefficient multiple interfacial charge transfer processes, the overall performance is only comparable to or mostly worse than the sole sensitizer-based devices.

Received: April 6, 2015
Published: April 16, 2015

DOI: 10.1021/acs.jpcc.5b03313
J. Phys. Chem. C 2015, 119, 9774−9781

In this study, we report a surprisingly effective approach, with which a judiciously designed relay molecule instead of a complex organic dye is grafted on the surface of CdS-sensitized TiO_2 electrode to instantaneously remove the photogenerated holes from CdS upon illumination, and block the recombination of injected electrons with cobalt-based electrolyte. As a result, photocorrosion of CdS is greatly prohibited and unprecedented cell performance is achieved with a significant enhancement of V_{OC}.

EXPERIMENTAL SECTION

Synthesis of 4′-(Bis(4-(hexyloxy)phenyl)amino)-biphenyl-4-carboxylic Acid (PAPC). All the chemicals for PAPC synthesis are received from Sigma-Aldrich. ^{1}H NMR and ^{13}C NMR spectra were characterized by Bruker AVANCE III-400 MHz (100 MHz for ^{13}C NMR) instruments with tetramethylsilane (TMS) as internal standard. The detailed synthetic procedure is elaborated on in the Supporting Information.

Preparation of the Photoanodes. A fluorine-doped tin oxide (FTO, Pilkington TEC-15, 15 Ω sq^{-1}) glass plate was cleaned by 5% Decon 90 solution, deionized water, and ethanol sequentially in an ultrasonic bath. A compact TiO_2 layer was synthesized onto that cleaned FTO glass by spray pyrolysis at 500 °C. A transparent mesoporous TiO_2 layer (90-T, Dyesol, ∼6 μm) and scattering layer (∼3 μm, no scattering layer for TA) were prepared onto the substrate by the screen-printing method. Thereafter, the electrode was gradually heated at 125 °C for 5 min, at 325 °C for 5 min, at 375 °C for 5 min, at 450 °C for 15 min, and at 500 °C for 15 min. Finally, the TiO_2 electrode was treated by 40 mM $TiCl_4$ aqueous solution at 70 °C for 30 min and then sintered at 500 °C for 30 min.

CdS was deposited onto the TiO_2 photoanodes by a successive ionic layer adsorption and reaction (SILAR) method.[14,27,28] Generally, the electrodes were first dipped into a 0.02 M cation precursor of cadmium nitrate ($Cd(NO_3)_2 \cdot 4H_2O$, Sigma-Aldrich, >99.0%) methanol solution for 1 min, rinsed with methanol for 1 min, and dried for 1 min with gentle flow of nitrogen gas. Then the electrodes were immersed into anion precursor solution containing 0.02 M sodium sulfide ($Na_2S \cdot 9H_2O$, Sigma-Aldrich, >98%) dissolved in a mixture of methanol and deionized water (1:1, v/v) for 1 min, rinsed with methanol for 1 min, and dried for 1 min with nitrogen gas. This completed one cycle. This SILAR procedure was repeated ten times. Thereafter, the CdS-sensitized TiO_2 was dipped into a 0.2 mM PAPC or stearic acid (SA, Sigma-Aldrich) acetonitrile solution for 24 h to adsorb enough relay or passivation molecules onto the electrode surface.

Solar Cell Fabrication. SSCs were assembled by separating the sensitized TiO_2 film and the platinized FTO glass with a hot-melt spacer (25 μm, Surlyn, DuPont) and followed by heating at 110 °C for 1 min. The platinized FTO counter electrode was prepared by thermal decomposition of hexachloroplatinic acid at 400 °C for 15 min. Then the cobalt−bipyridyl complex (0.2 M $[Co(bpy)_3](PF_6)_2$, 0.02 M $[Co(bpy)_3](PF_6)_3$, 0.5 M $LiClO_4$, and 0.5 M 4-*tert*-butylpyridine in acetonitrile) was injected through a hole at the platinized FTO under a partial vacuum. Finally, the hole was sealed with a small piece of hot-melt polymer and a cover glass.

Computational Details. A two-dimensional CdS (1 1 0) surface with 54 CdS in one unit cell was applied to simulate this semiconductor. All the calculations on the system with CdS were performed by using the plane-wave technique implemented in Vienna *ab initio* simulation package.[29,30] Generalized gradient approximation with the Perdew−Burke−Ernzerhof functional was employed in order to account for the electron exchange and correlation effects in all calculations.[29] The projector-augmented wave method has been applied to describe the electron−ion interactions, and the cutoff energy was set to 400 eV, which was chosen by total energy convergence calculation for CdS slab model.[30] The 5 × 5 × 1 Γ-centered k-point meshes were used structure optimization for the periodic systems. The frontier orbitals of the isolated PAPC molecule were calculated with density functional theory at the B3LYP/6-311G(d,p) level by Gaussian 09.

Characterizations. The thickness of TiO_2 film was determined with an Alpha-Step IQ surface profiler (KLA-Tencor). Absorbance spectra were measured by a UV−vis−NIR spectrophotometer (Shimadzu, Solidspec-3700). The cyclic voltammetry (CV) measurement was scanned in 0.1 M $LiClO_4$−acetonitrile solution with a reference of $Ag/AgNO_3$ and a counter of Pt wire at a rate of 100 mV s^{-1}. Electrochemical impedance spectroscopy (EIS) was measured from 10^6 to 0.1 Hz with a perturbation of 12 mV.

Photocurrent−voltage characteristics under AM 1.5G illumination at 95 mW cm^{-2} were carried out with a Keithley 2400 source meter and PVIV software package from Newport. The sunlight is obtained from a solar simulator (450 W, Newport class A), and the power was calibrated with a silicon reference cell. The active area of the cells was 0.12 cm^2 defined by a mask. The IPCE spectra were attained under a 300 W xenon lamp and a grating monochromator with a spectral resolution of ∼5 nm (Newport/Oriel) controlled by TRACQ basic software (Newport). The photostability test was determined under AM 1.5G illumination at 95 mW cm^{-2} for about 400 s with photocurrent or photovoltage recorded every 0.5 s by Autolab.

The carrier dynamics in the photoanodes was investigated by the ultrafast transient absorption and pump−probe experiments, which were performed by using a Ti:sapphire oscillator seeded regenerative amplifier system (Vitesse, Coherent). The output beam has a pulse duration of 60 fs, centered at 800 nm with a repetition rate of 1 kHz. Briefly, the 800 nm laser beam was split into two portions. A larger portion passed through an optical parametric amplifier (TOPAS-c, Light conversion) to generate a 500 nm beam to act as a pump beam. The pump beam was modulated by an optical chopper at a frequency of 500 Hz. A residual portion of the beam was used to generate white light continuum (WLC) in a 1 mm sapphire plate. The WLC was split into two beams: one as probe and the other as a reference to correct for pulse-to-pulse intensity fluctuations. The signal and reference beams were detected by photodiodes that are connected to lock-in amplifiers and the computer. The pump beam is focused onto the photoanode with a beam size of 300 μm and overlaps with the smaller diameter (100 μm) probe beam. The delay between the pump and probe pulses was varied by a computer-controlled translation stage (Newport, ESP 300). The variation transmittance at selected probe wavelength is recorded as a function of time delay between pump and probe pulses.

The cell was excited with a 532 nm laser beam from a Nd:YAG Q-switched laser (Continuum Minilite II). The pulse width is 5 ns, and the repetition rate is 5 Hz. The beam area after 3× beam expander is diameter 9 mm. This laser beam was illuminated onto the device together with the monochromatic probe light which is from IPCE system. Behind the device, there was a photodiode detector (Thorlabs FDS100, 10 ns rise

DOI: 10.1021/acs.jpcc.5b03313
J. Phys. Chem. C 2015, 119, 9774−9781

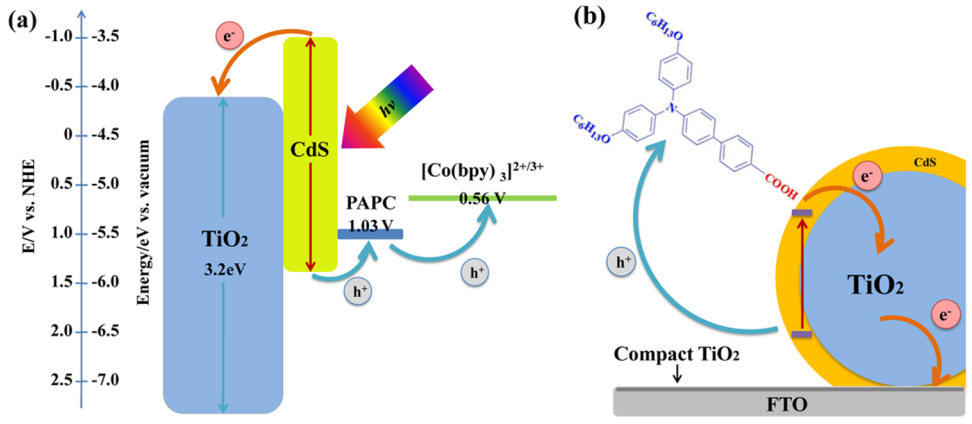

Figure 1. (a) Band diagram and charge separation processes of CdS/PAPC-sensitized TiO_2 photoanode. (b) Schematic illustrating CdS-sensitized TiO_2 electrode grafted with PAPC relay molecule on the surface of CdS.

time) working at 10 V reverse bias to record the transmitted light intensity, with a 532 nm notch filter positioned in front to reject stray light. An oscilloscope (Tektronix DPO2022B, 200 MHz bandwidth) and a current amplifier (FEMTO DHPCA-100, 80 MHz bandwidth) were controlled by Labview software to determine the photocurrent. Another photodiode equipped with an integrated current amplifier (PDA36A, Thorlabs) was operated for trigger. The TA measurement is carried out at open circuit condition, and the traces were averaged 512 times before analyzing these results with Mathematica 8. During the TA test, a mask slightly smaller than working area was coved onto the rear surface of the solar cells in order to make sure that only the probe light which passed though the devices can finally arrive at the photodiode detector.

RESULTS AND DISCUSSION

Triphenylamine derivatives have been extensively investigated as the donor moiety for D-pi-A organic sensitizers in DSCs,[6] particularly for those employing cobalt−bipyridyl complexes as the redox mediator, and revealed excellent charge separation property. Such configuration meanwhile effectively suppresses the recombination of injected electrons with the oxidized cobalt complexes in the electrolyte. Inspired by the D-pi-A structure, in this study we thus choose a triphenylamine derivative, 4′-(bis(4-(hexyloxy)phenyl)amino)biphenyl-4-carboxylic acid (PAPC), as the relay molecule. The carboxylic acid group anchors the molecule on the surface of chalcogenide semiconductor sensitizer, which has been confirmed to be feasible by several prior studies.[26,31−35] It is believed that PAPC will mostly adsorb on the surface of CdS given the conformal deposition of CdS on TiO_2 by the SILAR method,[28] while it is inevitable for some of the molecules to go onto the exposed TiO_2 surface. As illustrated in Figures 1a and 1b, the proposed charge transfer processes of the CdS/PAPC-sensitized solar cell are the following:

$$CdS + h\nu \rightarrow CdS(e^- + h^+) \quad (1)$$

$$CdS(e^- + h^+) + TiO_2 \rightarrow CdS(h^+) + TiO_2(e^-) \quad (2)$$

$$CdS(h^+) + PAPC \rightarrow CdS + PAPC^{\bullet+} \quad (3)$$

$$PAPC^{\bullet+} + [Co(bpy)_3]^{2+} \rightarrow PAPC + [Co(bpy)_3]^{3+} \quad (4)$$

Upon illumination, CdS absorbs photons to excite electrons to high-energy levels leaving holes in the valence band (VB) (eq 1). The excited electrons are then injected into TiO_2 (eq 2) and diffuse through the film before extracted to the external circuit. Meanwhile, since the energy level of the surface-grafted PAPC (HOMO 1.03 V vs NHE, LUMO −2.45 V vs NHE, see Figure S1) is higher than the VB maximum of CdS, PAPC will be oxidized to $PAPC^{\bullet+}$ by the holes transferred from CdS (eq 3). The formed $PAPC^{\bullet+}$ is then regenerated by $[Co(bpy)_3]^{2+}$ in the electrolyte, resulting in efficient charge separation (eq 4).

The charge transfer process between the grafted PAPC relay molecule and the underlying CdS is corroborated by theoretical calculations. Figure 2 shows the electron density difference map

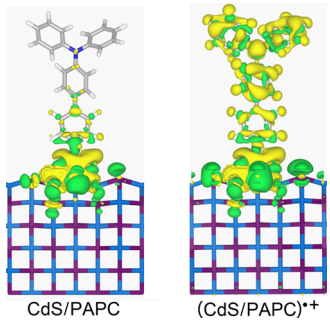

Figure 2. Electron density difference map associated with the interaction in CdS/PAPC and $(CdS/PAPC)^{\bullet+}$ system. Isovalues: | 0.000 35 aul. PAPC is adsorbed on the (110) surface of CdS QDs. The green and yellow zones correspond to electron density enhancement and deduction regions, respectively.

of CdS/PAPC as well as the $(CdS/PAPC)^{\bullet+}$ system where the green and yellow zones correspond to electron density enhancement and deduction regions, respectively. In dark, there is hardly redistribution of charges in CdS/PAPC indicating negligible charge transfer between CdS and PAPC. While under illumination, electrons in CdS VB are excited and then injected into TiO_2, leaving holes in CdS and forming $(CdS/PAPC)^{\bullet+}$. Significant charge redistribution is observed as a result of hole transfer from CdS to the HOMO of PAPC. The charge transfer is quantified by the Bader charge calculation to be 0.47 h^+ for $(CdS/PAPC)^{\bullet+}$, considerably higher than 0.03 h^+ for CdS/PAPC. In addition, as revealed in Figure S2, the orbital shape of CdS/PAPC system obtained from Γ-point frontier orbitals calculation shows clear fingerprint of the pure CdS and isolated PAPC, indicating negligible charge transfer between them under dark condition, which is consistent with the

DOI: 10.1021/acs.jpcc.5b03313
J. Phys. Chem. C 2015, 119, 9774−9781

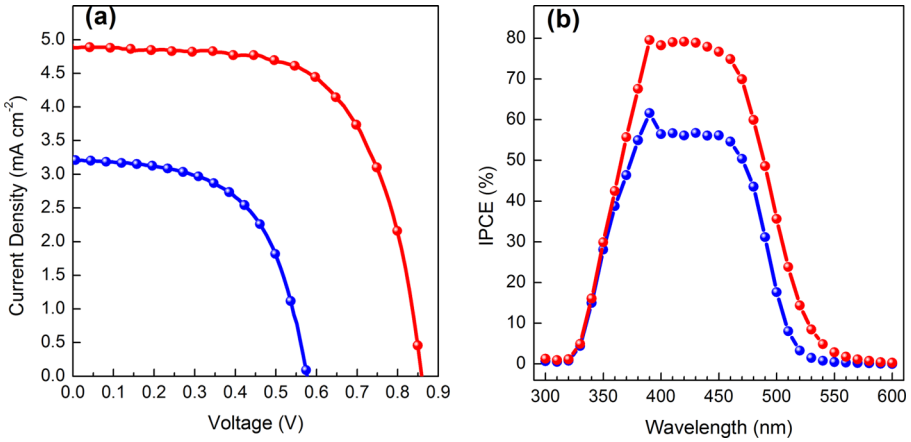

Figure 3. Photovoltaic performance of CdS (blue) and CdS/PAPC (red)-sensitized TiO_2 solar cells: (a) photocurrent−voltage characteristics under AM 1.5G, 0.95 sun illumination; (b) IPCE spectra. The electrolyte consists of 0.20 M $[Co(bpy)_3](PF_6)_2$, 0.02 M $[Co(bpy)_3](PF_6)_3$, 0.50 M $LiClO_4$, and 0.50 M 4-*tert*-butylpyridine in acetonitrile solution. The counter electrode is platinized FTO glass. The active working area is 0.12 cm^2 determined by a mask.

electron density difference and Bader charge results. Γ-point frontier orbitals of the CdS/PAPC system also suggests the energy $E_{CdS,VB} < E_{PAPC,HOMO} < E_{CdS,CB} < E_{PAPC,LUMO}$, being a typical type II band alignment between CdS and PAPC. Therefore, in the dark there is no obvious charge redistribution since the HOMO of the PAPC is lower than the CdS conduction band (CB), making it no driving force for the electron transfer. Under illumination, on the other hand, the leftover holes in CdS VB incline to transfer to the HOMO of PAPC due to the higher energy level of the latter. This is in line with the previous electron density difference and Bader charge calculations, suggesting favorable charge transfer between PAPC and CdS^+.

Figure 3a shows the photocurrent−voltage characteristics of the CdS- and CdS/PAPC-sensitized TiO_2 solar cells in $[Co(bpy)_3]^{2+/3+}$ electrolyte. The performance of CdS/TiO_2 cell is just mediocre while the V_{OC} is significantly lower than that of the dye-sensitized counterpart in the same electrolyte. In contrast, when the surface of CdS is grafted with PAPC, the cell performance is drastically enhanced, yielding a V_{OC} of 858 mV, J_{SC} of 4.91 mA cm^{-2}, and efficiency of 2.84% under AM 1.5G, 0.95 sun illumination, as summarized in Table 1. This

Table 1. Characteristics of CdS and CdS/PAPC-Sensitized TiO_2 Solar Cells under Simulated AM 1.5G, 95 mW cm^{-2} Illumination

sample	V_{OC} (V)	J_{SC} (mA cm^{-2})	fill factor (%)	efficiency (%)
CdS	0.576	3.21	58.1	1.13
CdS/PAPC	0.858	4.91	64.0	2.84

performance is also much superior to PAPC-sensitized cells, which typically have a V_{OC} of 849 mV, J_{SC} of 2.71 mA cm^{-2}, and efficiency of 1.32% (Figure S3). The incident photon-to-current conversion efficiency (IPCE, Figure 3b) of the CdS/PAPC-sensitized cell is close to 80% in a broad wavelength range, which is within a few percent of the transmission limit of the FTO substrate, indicating that light harvesting, charge separation, and charge collection are all close to unity for the PAPC grafted cells.

Cell stability is also considerably enhanced after surface modification with the relay molecule, as revealed in Figures S4a and S4b. Under short circuit conditions, both devices produced a normalized photocurrent close to 1 immediately after the shutter opened (at 10 s) but then dropped quickly to only 1% for QDSC without PAPC modification after 400 s of light soaking, which is in good contrast to 77% remained for the cell grafted with PAPC. Similarly under open circuit conditions, a relatively high photovoltage was kept almost unchanged for CdS/PAPC-sensitized solar cells, while in the absence of relay molecule, the cell voltage dropped continually with 76% left at 400 s. The enhanced stability makes it possible to investigate the CdS/PAPC-sensitized cells by using various frequency and time-resolved techniques, for insightful understanding of the charge transfer processes under illumination.

Electrochemical impedance spectroscopic (EIS) measurement was carried out in dark for cells with and without PAPC modification, as shown in Figure S5. The chemical capacitance (C_μ) and interfacial charge transfer resistance (R_{ct}) were obtained by fitting the spectra. The results reveal that the conduction band of TiO_2 shifts upward slightly upon grafting PAPC while R_{ct} increases considerably, resulting of a much longer electron lifetime in TiO_2 film. This is consistent with the much-enhanced V_{OC} after modifying with PAPC.

The underlying causes for the significant cell performance improvement could be understood by scrutinizing the elementary kinetic processes dictating cell operations, as implicated by the external quantum efficiency

$$\mathrm{IPCE}(\lambda) = \eta_{lh}(\lambda)\eta_{sep}(\lambda)\eta_{coll}(\lambda) \quad (5)$$

where η_{lh} is the light-harvesting efficiency, η_{sep} is the charge separation efficiency determined by the yields of electron injection (η_{inj}) and sensitizer regeneration (η_{reg}), and η_{coll} is the charge collection efficiency.[6,36] PAPC molecule itself has pale yellow color when adsorbed onto TiO_2 film. Because of the relatively low absorption coefficient, the peak absorbance of PAPC is only 1/6 of the CdS in TiO_2/CdS/PAPC cell (Figure 4). This indicates, to a first approximation, that the photocurrent generated by PAPC would be far less than that of CdS. In addition, considering that for those PAPC molecules grafted on CdS, electron injection into TiO_2 will have to go through the CdS phase during which there is an additional chance of recombination, the photocurrent generation by PAPC would be even less efficient than that by CdS. Hence, contribution of the PAPC relay molecules to light harvesting would only be

DOI: 10.1021/acs.jpcc.5b03313
J. Phys. Chem. C 2015, 119, 9774−9781

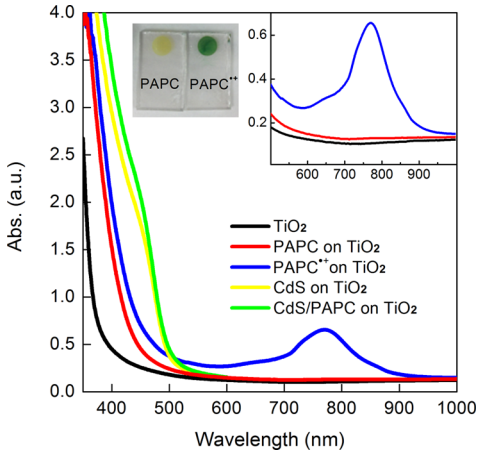

Figure 4. Absorbance spectra of a TiO_2 electrode (black) after adsorbing PAPC (red) or depositing CdS (yellow) and CdS/PAPC (green). The insets highlight the peak position of $PAPC^{\bullet+}$ (blue) and photos of these two electrodes.

marginal in CdS/PAPC-sensitized TiO_2 cells, and η_{lh} would not be the main reason for the significant enhancement of IPCE. Thus, the improvement must stem from improved charge separation or/and collection.

There is another possibility that the improvement is a result of better passivation of both CdS and exposed TiO_2 surface, which enhances charge collection and boosts photovoltage. In order to investigate the "passivation effect", stearic acid (SA) was grafted onto CdS surface. The length of this molecule is similar to PAPC. In addition, it is also the carboxylic group that anchors onto CdS and TiO_2. The only difference is that SA does not bear redox activity. The photovoltaic characteristics of the cells are shown in Figure S6 and Table S1. Clearly, the presence of SA molecule on CdS-sensitized TiO_2 electrode does not enhance the cell performance. Although the photovoltage is slightly improved as a result of passivation, both the photocurrent and fill factor become deteriorated, which lead to an even reduced power conversion efficiency. In addition, the presence of SA molecule does not effectively improve the stability of CdS-sensitized TiO_2 cell, either, indicating the passivation effect is not a dominating factor for the enhanced device performance. One may argue that SA has poorer passivation than PAPC. But it is noteworthy that similar molecule has been employed in DSC, which revealed beneficial effect in the same cobalt−bipyridyl complex-based electrolyte.[37] So in contrast to the PAPC relay molecule, SA molecule seems to just modestly prevent charge recombination as an insulating barrier layer, which clearly indicates that passivation is insignificant or at least not a dictating factor to the overall performance enhancement of the cell. Based on the above analysis, the "relay effect" with facilitated charge separation seemingly plays a more important role than enhanced light harvesting and passivation effect.

$PAPC^{\bullet+}$ is a green color radical cation with an absorption peak at ~770 nm (inset of Figure 4), while CdS^+ has no specific absorption peak from 650 to 800 nm (Figure S7). The different evolutions of transient absorption spectra (TAS) can be measured to probe the concentration changes of $PAPC^{\bullet+}$ in CdS/PAPC-sensitized photoanodes upon illumination, so as to obtain information on the hole injection and regeneration processes. As revealed in Figure 5a, upon excited at 500 nm, which is transparent to both TiO_2 and PAPC, a broad absorption band centered at ~770 nm rises at time <1 ps and decays slowly at longer time. The time evolution of the absorption at 770 nm is shown in Figure 5b. The fast drop is probably due to the trapping dynamics of charges in CdS, where many surface states exist.[38] The formation of this new absorption band at 770 nm suggests that a population of new species is generated after laser excitation. Since the TAS profile just resembles that of the absorption spectrum of $PAPC^{\bullet+}$ (Figure 4), we attribute it to the production of $PAPC^{\bullet+}$ as a result of hole injection from CdS^+ into the surface grafted PAPC. As such, the hole injection rate from CdS^+ to PAPC could approximately be obtained by the rising edge in Figure 5b, which is faster than 1 ps. This time constant suggests that the hole in CdS VB can be transferred to PAPC in subpicosecond time scale after laser excitation, which is comparable to the hole transfer rate from CdSe to Na_2S based electrolyte,[39] and to the rate in CdS−dibromofluorescein supersensitized system.[38] The regeneration time constant cannot be obtained from the time trace in Figure 5b because the process is much slower than 1000 ps. In order to get more accurate time constant for the regeneration reaction, nanosecond TA was carried out, which is shown in Figure 6.

Similar to the femtosecond laser measurement, a peak at ~770 nm was also observed in the nanosecond TAS after excited by 532 nm laser pulse, which was attributed to the

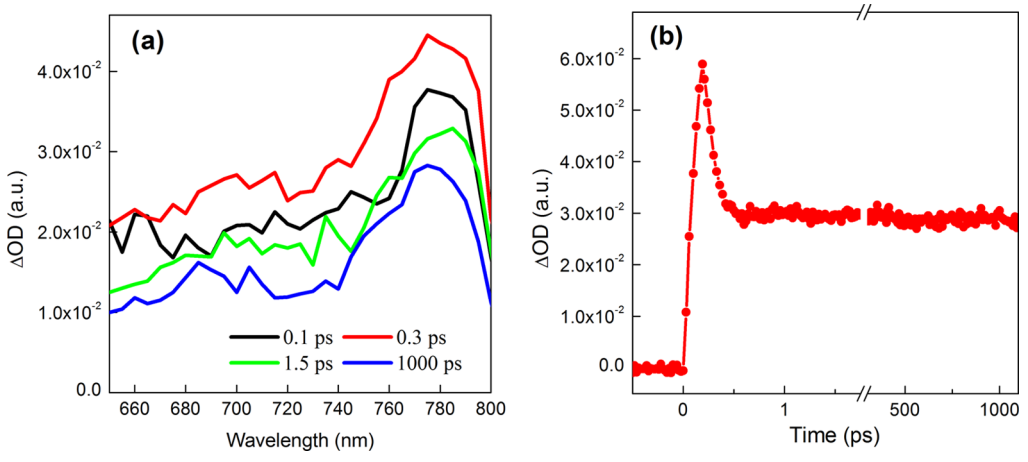

Figure 5. Transient absorption spectra during 0.1−1000 ps (a) and time trace at 770 nm (b) of a CdS/PAPC-sensitized TiO_2 solar cell.

DOI: 10.1021/acs.jpcc.5b03313
J. Phys. Chem. C 2015, 119, 9774−9781

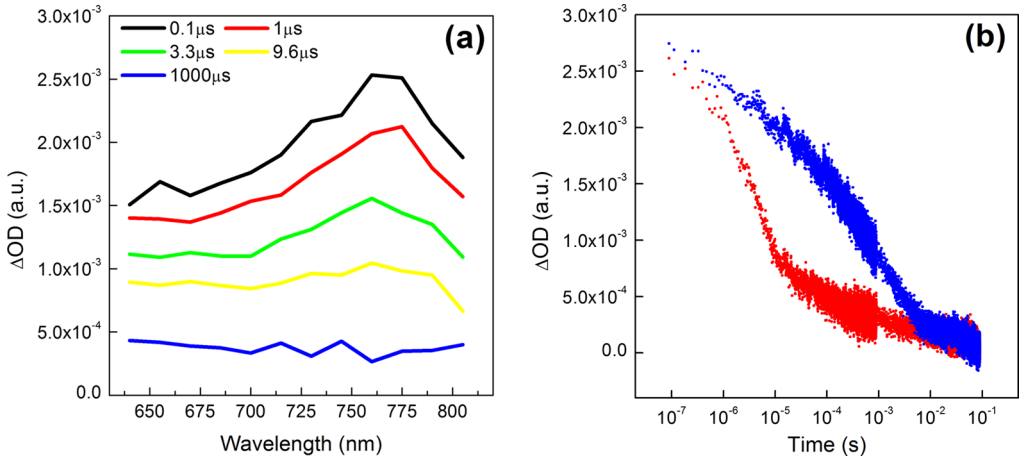

Figure 6. (a) Transient absorption spectra during 100 ns ∼1 ms of CdS/PAPC-sensitized solar cells. (b) Time trace at 770 nm of normal cell (red) and blank cell (blue). The electrolyte of normal cell consists of 0.20 M $[Co(bpy)_3](PF_6)_2$, 0.02 M $[Co(bpy)_3](PF_6)_3$, 0.50 M $LiClO_4$, and 0.50 M 4-*tert*-butylpyridine, while the blank cell consists of 0.46 M EMITFSI, 0.50 M $LiClO_4$, and 0.50 M 4-*tert*-butylpyridine.

absorption of $PAPC^{\bullet+}$ (Figure 6a). The fitting of TA trace at 770 nm (Figure 6b) is however complicated by nontrivial absorption of electrons in both CdS and TiO_2 at 770 nm at this time scale as well as limited features in Figure 6b to differentiate the decay of $PAPC^{\bullet+}$ and e^-. As such, we measured the TA of a blank cell (without redox species), as shown in Figure 6b, to determine the geminate recombination kinetics between $PAPC^{\bullet+}$ and electrons in TiO_2/CdS, so that we could obtain the time constant for $PAPC^{\bullet+}$ regeneration. The geminate recombination time constant is around 10^{-4}–10^{-2} s, with which the regeneration time constant of $PAPC^{\bullet+}$ was semiquantitatively estimated to be around 10^{-6}–10^{-4} s, very close to the regeneration time constant in DSCs employing D-pi-A dyes and $[Co(bpy)_3]^{2+/3+}$-based electrolyte.[36] This is not surprising considering similar triarylamine donor moiety and cobalt complex were used in both cases.

The above measurement has drawn a clear picture of the charge transfer processes in CdS/PAPC-sensitized solar cells. Upon illumination, the photogenerated holes in the CdS VB are instantaneously removed by the surface-grafted PAPC relay molecule, which has multiple effects on the operation of solar cells: (1) The immediate effect is that high energy holes are rapidly removed from CdS QDs, photocorrosion of the material is thus alleviated. (2) Holes are spatially further separated from the injected electrons in TiO_2, so geminate recombination is suppressed. (3) The structure of PAPC is proved to be effective in impeding the recombination of injected electrons with $[Co(bpy)_3]^{2+/3+}$-based electrolyte. As a result, both charge separation and collection of the cells are considerably improved, which adequately interprets the enhancement of photocurrent. Moreover, the high photovoltage of CdS/PAPC-sensitized devices is well supported by the retarded recombinations of injected electrons in the presence of molecular relay. Consequently, the overall power conversion efficiency of the cells is significantly improved.

CONCLUSIONS

In conclusion, a novel design for high efficiency and stability semiconductor-sensitized solar cell is developed by grafting redox relay molecule on the surface of the semiconductor sensitizer. In this particular case, a triarylamine derivative PAPC molecule with redox potential lower than CdS VB while higher than the redox electrolyte was adsorbed on CdS-sensitized TiO_2 electrode which exhibits surprisingly better photovoltaic characteristics in $[Co(bpy)_3]^{2+/3+}$-based electrolyte. Transient absorption measurement indicates that the photogenerated holes reside in CdS only for <1 ps before they are transferred into the surface grafted PAPC molecules. This instantaneous interception of holes from CdS VB greatly enhances the charge separation and stabilizes the QDs in $[Co(bpy)_3]^{2+/3+}$-based electrolyte and consequently results in an unprecedented power conversion efficiency.

It is believed that with suitable redox relay molecules the concept could be feasibly applied to other semiconductor sensitizer, especially for those having superior long wavelength light absorption, such as CdSe and CdTe, etc. We anticipate that the concept presented here provide a valuable approach for the development of high-efficiency and stability semiconductor-sensitized solar cells.

ASSOCIATED CONTENT

Supporting Information

Cyclic voltammograms of CdS/PAPC-sensitized TiO_2 photoanode; absorbance spectrum of PAPC in acetonitrile; Γ-point frontier orbitals of CdS/PAPC, pure CdS, and isolate PAPC molecule system; photovoltaic performance of PAPC-sensitized TiO_2 solar cells; photostability of CdS- and CdS/PAPC-sensitized solar cells; EIS results of CdS and CdS/PAPC-sensitized TiO_2 solar cell in dark; photovoltaic and photostability performance of CdS and CdS/SA-sensitized TiO_2 solar cells; TAS of a CdS-sensitized TiO_2 solar cell; synthetic method of PAPC; statistic photovoltaic performance of the solar cells. This material is available free of charge via the Internet at http://pubs.acs.org.

AUTHOR INFORMATION

Corresponding Author

*E-mail qing.wang@nus.edu.sg; Tel +65 65167118; Fax +65 67763604 (Q.W.).

Notes

The authors declare no competing financial interest.

DOI: 10.1021/acs.jpcc.5b03313
J. Phys. Chem. C 2015, 119, 9774–9781

■ ACKNOWLEDGMENTS

This research is supported by National Research Foundation Singapore under the SinBeRISE program and MOE AcRF grant (R-143-000-495-112 and R-143-000-533-112).

■ REFERENCES

(1) Kamat, P. V. Quantum Dot Solar Cells. The Next Big Thing in Photovoltaics. *J. Phys. Chem. Lett.* **2013**, *4*, 908−918.
(2) Nozik, A. J. Quantum Dot Solar Cells. *Physica E* **2002**, *14*, 115−120.
(3) Ruhle, S.; Shalom, M.; Zaban, A. Quantum-Dot-Sensitized Solar Cells. *ChemPhysChem* **2010**, *11*, 2290−2304.
(4) Mora-Seró, I.; Bisquert, J. Breakthroughs in the Development of Semiconductor-Sensitized Solar Cells. *J. Phys. Chem. Lett.* **2010**, *1*, 3046−3052.
(5) O'Regan, B.; Gratzel, M. A Low-Cost, High-Efficiency Solar Cell Based on Dye-Sensitized Colloidal TiO_2 Films. *Nature* **1991**, *353*, 737−740.
(6) Hagfeldt, A.; Boschloo, G.; Sun, L.; Kloo, L.; Pettersson, H. Dye-Sensitized Solar Cells. *Chem. Rev.* **2010**, *110*, 6595−6663.
(7) Yella, A.; Lee, H. W.; Tsao, H. N.; Yi, C.; Chandiran, A. K.; Nazeeruddin, M. K.; Diau, E. W. G.; Yeh, C. Y.; Zakeeruddin, S. M.; Gratzel, M. Porphyrin-Sensitized Solar Cells with Cobalt (II/III)-Based Redox Electrolyte Exceed 12% Efficiency. *Science* **2011**, *334*, 629−634.
(8) Mathew, S.; Yella, A.; Gao, P.; Humphry-Baker, R.; CurchodBasile, F. E.; Ashari-Astani, N.; Tavernelli, I.; Rothlisberger, U.; NazeeruddinMd, K.; Grätzel, M. Dye-Sensitized Solar Cells with 13% Efficiency Achieved through the Molecular Engineering of Porphyrin Sensitizers. *Nat. Chem.* **2014**, *6*, 242−247.
(9) Yu, W. W.; Qu, L.; Guo, W.; Peng, X. Experimental Determination of the Extinction Coefficient of CdTe, CdSe, and CdS Nanocrystals. *Chem. Mater.* **2003**, *15*, 2854−2860.
(10) Sukhovatkin, V.; Hinds, S.; Brzozowski, L.; Sargent, E. H. Colloidal Quantum-Dot Photodetectors Exploiting Multiexciton Generation. *Science* **2009**, *324*, 1542−1544.
(11) Midgett, A. G.; Luther, J. M.; Stewart, J. T.; Smith, D. K.; Padilha, L. A.; Klimov, V. I.; Nozik, A. J.; Beard, M. C. Size and Composition Dependent Multiple Exciton Generation Efficiency in PbS, PbSe, and PbS_XSe_{1-X} Alloyed Quantum Dots. *Nano Lett.* **2013**, *13*, 3078−3085.
(12) Zaban, A.; Micic, O. I.; Gregg, B. A.; Nozik, A. J. Photosensitization of Nanoporous TiO_2 Electrodes with InP Quantum Dots. *Langmuir* **1998**, *14*, 3153−3156.
(13) Niitsoo, O.; Sarkar, S. K.; Pejoux, C.; Ruhle, S.; Cahen, D.; Hodes, G. Chemical Bath Deposited CdS/CdSe-Sensitized Porous TiO_2 Solar Cells. *J. Photochem. Photobiol., A* **2006**, *181*, 306−313.
(14) Shen, C.; Sun, L.; Koh, Z. Y.; Wang, Q. Cuprous Sulfide Counter Electrodes Prepared by Ion Exchange for High-efficiency Quantum Dot-Sensitized Solar Cells. *J. Mater. Chem. A* **2014**, *2*, 2807.
(15) Wang, J.; Mora-Sero, I.; Pan, Z.; Zhao, K.; Zhang, H.; Feng, Y.; Yang, G.; Zhong, X.; Bisquert, J. Core/Shell Colloidal Quantum Dot Exciplex States for the Development of Highly Efficient Quantum-Dot-Sensitized Solar Cells. *J. Am. Chem. Soc.* **2013**, *135*, 15913−15922.
(16) Luo, J.; Wei, H.; Huang, Q.; Hu, X.; Zhao, H.; Yu, R.; Li, D.; Luo, Y.; Meng, Q. Highly Efficient Core-Shell $CuInS_2$-Mn Doped CdS Quantum Dot Sensitized Solar Cells. *Chem. Commun.* **2013**, *49*, 3881−3883.
(17) Hod, I.; González-Pedro, V.; Tachan, Z.; Fabregat-Santiago, F.; Mora-Seró, I.; Bisquert, J.; Zaban, A. Dye versus Quantum Dots in Sensitized Solar Cells: Participation of Quantum Dot Absorber in the Recombination Process. *J. Phys. Chem. Lett.* **2011**, *2*, 3032−3035.
(18) Feldt, S. M.; Wang, G.; Boschloo, G.; Hagfeldt, A. Effects of Driving Forces for Recombination and Regeneration on the Photovoltaic Performance of Dye-Sensitized Solar Cells Using Cobalt Polypyridine Redox Couples. *J. Phys. Chem. C* **2011**, *115*, 21500−21507.
(19) Liu, Y.; Jennings, J. R.; Huang, Y.; Wang, Q.; Zakeeruddin, S. M.; Grätzel, M. Cobalt Redox Mediators for Ruthenium-Based Dye-Sensitized Solar Cells: A Combined Impedance Spectroscopy and Near-IR Transmittance Study. *J. Phys. Chem. C* **2011**, *115*, 18847−18855.
(20) Yum, J. H.; Baranoff, E.; Kessler, F.; Moehl, T.; Ahmad, S.; Bessho, T.; Marchioro, A.; Ghadiri, E.; Moser, J. E.; Yi, C.; et al. A Cobalt Complex Redox Shuttle for Dye-Sensitized Solar Cells with High Open-Circuit Potentials. *Nat. Commun.* **2012**, *3*, 631.
(21) Shen, H.; Li, J.; Zhao, L.; Zhang, S.; Wang, W.; Oron, D.; Lin, H. Synergistic Recombination Suppression by an Inorganic Layer and Organic Dye Molecules in Highly Photostable Quantum Dot Sensitized Solar Cells. *Phys. Chem. Chem. Phys.* **2014**, *16*, 6250−6256.
(22) Roelofs, K. E.; Brennan, T. P.; Dominguez, J. C.; Bailie, C. D.; Margulis, G. Y.; Hoke, E. T.; McGehee, M. D.; Bent, S. F. Effect of Al_2O_3 Recombination Barrier Layers Deposited by Atomic Layer Deposition in Solid-State CdS Quantum Dot-Sensitized Solar Cells. *J. Phys. Chem. C* **2013**, *117*, 5584−5592.
(23) Shalom, M.; Dor, S.; Rühle, S.; Grinis, L.; Zaban, A. Core/CdS Quantum Dot/Shell Mesoporous Solar Cells with Improved Stability and Efficiency Using an Amorphous TiO_2 Coating. *J. Phys. Chem. C* **2009**, *113*, 3895−3898.
(24) Rühle, S.; Greenshtein, M.; Chen, S. G.; Merson, A.; Pizem, H.; Sukenik, C. S.; Cahen, D.; Zaban, A. Molecular Adjustment of the Electronic Properties of Nanoporous Electrodes in Dye-Sensitized Solar Cells. *J. Phys. Chem. B* **2005**, *109*, 18907−18913.
(25) Shalom, M.; Rühle, S.; Hod, I.; Yahav, S.; Zaban, A. Energy Level Alignment in CdS Quantum Dot Sensitized Solar Cells Using Molecular Dipoles. *J. Am. Chem. Soc.* **2009**, *131*, 9876−9877.
(26) Choi, H.; Nicolaescu, R.; Paek, S.; Ko, J.; Kamat, P. V. Supersensitization of CdS Quantum Dots with a Near-Infrared Organic Dye: Toward the Design of Panchromatic Hybrid-Sensitized Solar Cells. *ACS Nano* **2011**, *5*, 9238−9245.
(27) Lee, H.; Wang, M.; Chen, P.; Gamelin, D. R.; Zakeeruddin, S. M.; Grätzel, M.; Nazeeruddin, M. K. Efficient CdSe Quantum Dot-Sensitized Solar Cells Prepared by an Improved Successive Ionic Layer Adsorption and Reaction Process. *Nano Lett.* **2009**, *9*, 4221−4227.
(28) Hossain, M. A.; Jennings, J. R.; Shen, C.; Pan, J. H.; Koh, Z. Y.; Mathews, N.; Wang, Q. CdSe-Sensitized Mesoscopic TiO_2 Solar Cells Exhibiting >5% Efficiency: Redundancy of CdS Buffer Layer. *J. Mater. Chem.* **2012**, *22*, 16235.
(29) Perdew, J. P.; Burke, K.; Ernzerhof, M. Generalized Gradient Approximation Made Simple. *Phys. Rev. Lett.* **1996**, *77*, 3865−3868.
(30) Blöchl, P. E. Projector Augmented-Wave Method. *Phys. Rev. B* **1994**, *50*, 17953−17979.
(31) Celebi, S.; Erdamar, A. K.; Sennaroglu, A.; Kurt, A.; Acar, H. Y. Synthesis and Characterization of Poly(acrylic acid) Stabilized Cadmium Sulfide Quantum Dots. *J. Phys. Chem. B* **2007**, *111*, 12668−12675.
(32) Mora-Sero, I.; Gross, D.; Mittereder, T.; Lutich, A. A.; Susha, A. S.; Dittrich, T.; Belaidi, A.; Caballero, R.; Langa, F.; Bisquert, J.; et al. Nanoscale Interaction Between CdSe or CdTe Nanocrystals and Molecular Dyes Fostering or Hindering Directional Charge Separation. *Small* **2010**, *6*, 221−225.
(33) Fritzinger, B.; Capek, R. K.; Lambert, K.; Martins, J. C.; Hens, Z. Utilizing Self-Exchange To Address the Binding of Carboxylic Acid Ligands to CdSe Quantum Dots. *J. Am. Chem. Soc.* **2010**, *132*, 10195−10201.
(34) Mansur, H. S.; Mansur, A. A. P.; González, J. C. Synthesis and Characterization of CdS Quantum Dots with Carboxylic-Functionalized Poly(vinyl alcohol) for Bioconjugation. *Polymer* **2011**, *52*, 1045−1054.
(35) Choi, H.; Kamat, P. V. CdS Nanowire Solar Cells: Dual Role of Squaraine Dye as a Sensitizer and a Hole Transporter. *J. Phys. Chem. Lett.* **2013**, *4*, 3983−3991.
(36) Li, F.; Jennings, J. R.; Wang, Q. Determination of Sensitizer Regeneration Efficiency in Dye-Sensitized Solar Cells. *ACS Nano* **2013**, *7*, 8233−8242.

DOI: 10.1021/acs.jpcc.5b03313
J. Phys. Chem. C 2015, 119, 9774−9781

(37) Liu, Y.; Jennings, J. R.; Wang, X.; Wang, Q. Significant Performance Improvement in Dye-Sensitized Solar Cells Employing Cobalt(III/II) Tris-bipyridyl Redox Mediators by Co-grafting Alkyl Phosphonic Acids with a Ruthenium Sensitizer. *Phys. Chem. Chem. Phys.* **2013**, *15*, 6170−6174.
(38) Maity, P.; Debnath, T.; Ghosh, H. N. Ultrafast Hole- and Electron-Transfer Dynamics in CdS−Dibromofluorescein (DBF) Supersensitized Quantum Dot Solar Cell Materials. *J. Phys. Chem. Lett.* **2013**, *4*, 4020−4025.
(39) Shen, Q.; Ayuzawa, Y.; Katayama, K.; Sawada, T.; Toyoda, T. Separation of Ultrafast Photoexcited Electron and Hole Dynamics in CdSe Quantum Dots Aadsorbed onto Nanostructured TiO_2 Films. *Appl. Phys. Lett.* **2010**, *97*, 263113.

DOI: 10.1021/acs.jpcc.5b03313
J. Phys. Chem. C 2015, 119, 9774−9781